

See discussions, stats, and author profiles for this publication at: <https://www.researchgate.net/publication/334636774>

Experimental evaluation of activated carbon derived from South Africa discard coal for natural gas storage

Article · July 2019

DOI: 10.1007/s40789-019-0262-5

CITATIONS

0

5 authors, including:



Jibril Abdulsalam

University of the Witwatersrand

8 PUBLICATIONS 1 CITATION

[SEE PROFILE](#)



B.O. Oboirien

University of Johannesburg

38 PUBLICATIONS 241 CITATIONS

[SEE PROFILE](#)

READS

107



Lubilanji Jean Mulopo

University of the Witwatersrand

49 PUBLICATIONS 74 CITATIONS

[SEE PROFILE](#)



Samson Oluwaseyi Bada

University of the Witwatersrand

35 PUBLICATIONS 164 CITATIONS

[SEE PROFILE](#)

Some of the authors of this publication are also working on these related projects:



Ionic Liquids for CO₂ Capture [View project](#)



Hortus Capensis - donated the bamboo used in this research [View project](#)

Experimental evaluation of activated carbon derived from South Africa discard coal for natural gas storage

Jibril Abdulsalam^{1,2} · Jean Mulopo¹ · Bilainu Oboirien³ · Samson Bada² · Rosemary Falcon²

Received: 5 December 2018 / Revised: 26 June 2019 / Accepted: 11 July 2019
© The Author(s) 2019

Abstract Lacking in literature is the use of discard coal to produce activated carbon and in its subsequent use in the storage of natural gas. In this study, the characterization and gas storage evaluation of a largely porous activated carbon with large surface area synthesized from discard coal were investigated. Discard coals are waste material generated from coal beneficiation process. In developing the activated carbon, chemical activation route with the use of KOH reagent was applied. The effects of KOH/discard coal weight ratio (1:1, 2.5:1, 4:1), temperature (400–800 °C) and particle size (0.15–0.25 mm, 0.25–0.5 mm, 0.5–1 mm) on the adsorptive properties of the activated carbon were methodically evaluated and optimized using response surface methodology. The synthesized activated carbon was characterized using BET, SEM/EDS, and XRD. The results showed that for each activation process, the surface area and pore volume of the resulting activated carbon increased with increased temperature and KOH/discard coal weight ratio. The maximum surface area of 1826.41 m²/g, pore volume of 1.252 cm³/g and pore size of 2.77 nm were obtained at carbonization temperature of 800 °C and KOH/discard coal weight ratio of 4:1. Methane and nitrogen adsorption data at high pressure were fitted to Toth isotherm model with a predictive accuracy of about 99%. Adsorption parameters using the Toth model provides useful information in the design of adsorbed natural gas storage system. According to the requirements of adsorbent desired for natural gas storage, it could be stated that the synthesized activated carbon could well be applied for natural gas storage.

Keywords Discard coal · Activated carbon · Surface area · Methane · Adsorption

1 Introduction

The depletion of traditional oil reserves coupled with political uncertainty and environmental concerns have driven, in the past decade, a growing interest in gaseous fuel namely hydrogen and natural gas. Though these gaseous fuels are much less polluting than traditional fuels, they have low density hence there is a need to condense them to the maximum in order to optimize their storage. The adsorption of gaseous fuel on microporous materials for storage offers several supportive arguments (Lozano-Castello et al. 2002a; Celzard and Fierro 2005; Morris and Wheatley 2008; Makal et al. 2012). However, methane which is the major constituent of natural gas is supercritical at room temperature, and its adsorption does not necessarily lead to a condensed phase and in most cases requires the presence of narrow porosity such as slit pores (Makal

✉ Jean Mulopo
jean.mulopo@wits.ac.za

¹ Sustainable Energy and Environment Research Group, School of Chemical and Metallurgical Engineering, University of the Witwatersrand, Private Bag X3, Johannesburg WITS 2050, South Africa

² Clean Coal and Sustainable Energy Research Group, Faculty of Engineering and the Built Environment, University of the Witwatersrand, Private Bag X3, Johannesburg WITS 2050, South Africa

³ Department of Chemical Engineering, University of Johannesburg, Doornfontein, Johannesburg 2028, South Africa

et al. 2012). It has been shown in previous studies that carbonaceous materials, particularly activated carbons, can be prepared to satisfy this requirement.

In South Africa, exploring the energy potential of discard coal has been a challenge and a major concern to the Mining Companies and the Department of Mineral and Energy (DME). Discard coal are waste material generated from coal beneficiation process. Discard coal are produced as tailings which is less coarse coal from washing and fines from screening process (Piechura 2014). There is an accumulated 1.5 billion tons of discard coal stockpile in South Africa and 60 million tons produced annually (Belaïd et al. 2013). An aerial view of a stockpile of discard coal at Mpumalanga Highveld, South Africa is shown in Fig. 1. The problem of stockpiling discard coal on the environment include leaching, spontaneous combustion, the release of toxic substances and occupation of useful land space (Onifade and Genc 2018; Mills 2018). Therefore, there is an urgent need to find a beneficial use for discard coal.

Carbonaceous raw materials with high carbon composition are adjudged good starting material in preparing activated carbons. Widely used raw materials in activated carbon production are coconut shell, coal and wood (Bandosz and Ania 2006; Lillo-Ródenas et al. 2003; Torregrosa-Rodríguez et al. 2000). Various literature has reported the use of coal in activated carbon production (Sun et al. 1997; Hsu and Teng 2000; Himeno et al. 2005; Jibril et al. 2007; Martin et al. 2017; Gao et al. 2017). Lacking in literature is the use of discard coal to produce activated carbon for natural gas storage.

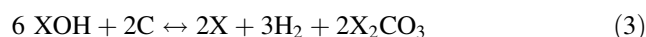
Physical and chemical activation processes are the two conventional methods used in the preparation of activated carbons. The physical activation process involves the

carbonization of the raw material followed by activation of the char produced using steam or carbon dioxide (CO_2) in accordance with the following reactions:



Equations (1) and (2) is the chemical conversion of carbon in the raw material during the physical activation process with the use of steam or CO_2 (Linares-Solano et al. 2012).

In contrast, chemical activation involves the use of chemical reagents such as potassium hydroxide (KOH), sodium hydroxide (NaOH), zinc chloride (ZnCl_2) and phosphoric acid (H_3PO_4). Chemical activation is a one-step process that produces activated carbon of well-developed porosity. The following reaction represents the chemical conversion that takes place during the chemical activation process using hydroxide:



where X: K, Na.

Generally, the chemical activation process has benefits of lower temperature, one-step process, higher yield, higher surface area and porosity than the physical activation process (Linares-Solano et al. 2012). The disadvantages of the process include an additional washing process and the corrosive nature of the chemical reagents.

The remarkable adsorptive capacity of activated carbons can be attributed to its tunable features such as surface area and porosity. These properties can be optimized to meet specific applications. For viability of natural gas use in vehicles, the US Department of Energy (DOE) evaluated deliverable capacity of a tank filled to 3.5 MPa and operating at 25 °C to 150 v/v (volume of gas per volume of tank) (Schroeder 2015) while a storage volume efficiency



Fig. 1 Aerial view of a stockpile of coal discard at Mpumalanga Highveld, South Africa (Center for Environmental Rights 2015)

of 80–100 v/v at ambient temperature and pressure of 3.5 MPa was recommended as appropriate for bulk storage of natural gas (Judd et al. 1998). To achieve this goal, many carbon-based adsorbents have been studied, and they appear to offer remarkable assets such as high density, low cost, and ease of activation. How much natural gas is stored is highly dependent on the textural characteristics of the activated carbons (Alcañiz-Monge et al. 2009). A suitable activated carbon to store natural gas should, therefore, possess the following characteristics:

- (1) A surface area greater than 1000 m²/g (Blanco et al. 2010).
- (2) Large microporosity to increase adsorption capacity (Marsh and Reinoso 2006).
- (3) The narrow pore size distribution of about 8 Å (Matranga et al. 1992).
- (4) Low mesoporosity to ease the kinetics of adsorption and desorption processes (Marsh and Reinoso 2006).

Achieving the aforementioned characteristics is dependent on the choice of raw material and the activation process. Available studies on discard coal are focused on improving the quality of discard for electricity production (Piechura 2014; North et al. 2015; Belaid et al. 2013). From available studies on discard coal, none has evaluated the potential of activated carbon derived from discard coal for gas storage application. This study looks at the opportunity offered by the significant amount of usable carbon in discard coal to produce activated carbon from discard coal as an adsorbent for natural gas storage.

2 Materials and methods

2.1 Materials and preparation

Discard coal sample was collected from a Mine situated 15 km south-west of Witbank in Mpumalanga, South Africa. The sample was dried under laboratory condition for 48 h. After drying, the sample was pulverized and sieved to varying particle sizes of 0.15–0.25 mm, 0.25–0.5 mm and 0.5–1.0 mm. The sample was physically mixed with chemical reagent at different weight ratio. The mixed samples were placed in a furnace and heated at 10 °C/min to a final temperature under a nitrogen flow of 100 ml/min STP. At the final temperature, the samples were held for 2 h, then cooled under nitrogen flow. The activated samples were washed using 0.5 N HCl to remove residual alkali (Wu et al. 2005). The samples were subsequently washed with distilled water and centrifuged until the pH of the sample and distilled water solution was 6 (Hu and Srinivasan 1999). The washed sample was kept in an oven at 110 °C overnight to dry. The dried activated

carbon was stored in sample bottles for subsequent analysis and characterization. The setup for the experiment is as shown in Fig. 2.

2.2 Analytical methods for discard coal characterization

Proximate analysis was conducted in accordance with the ISO 11722, 1171 and 562 standards. Approximately 1 g of each sample was used for the analyses in determining the inherent moisture, ash content and volatile matter present, with fixed carbon calculated by difference. The total sulfur and carbon in the discard coal were analyzed in accordance with ISO 12902 standard. Approximately 0.25 g of each sample was used for the analyses at a temperature up to 1450 °C with analysis time between 60 and 300 s.

2.3 Experiment design and statistical analysis

The experiment was designed using Design-Expert software (version 7.0.0) by Stat-Ease, Inc. Central composite design (CCD) component of the software was used to apply the response surface methodology (RSM) (Zhao et al. 2011) and to determine the number of experiments to be carried out. Two factors were examined in this study; KOH/discard coal weight ratio (*W*) and activation temperature (*T*). A total number of 13 experimental runs were obtained. The structure and design matrix of the experimental design is as shown in Table 1. There are four factorial points, four axial points, and five center points which were repeated five times to obtain an accurate estimate of experimental error. The significance of *W* and *T* in addition to their interactions were evaluated using analysis of variance (ANOVA). Statistical tools such as sum of squares, degrees of freedom, mean square, *p* value, *F*-value, correlation coefficient (*R*²), adjusted correlation coefficient (adj. *R*²) and predicted correlation coefficient (pred. *R*²) were used to evaluate the measured values from the experiment and the correlation with model predicted values.

2.4 Principle of material characterization and models used in this study

The structural characterization of porous material is important before its usage in an application such as natural gas storage. Gas adsorption techniques have been adjudged to be successful in characterizing porous materials such as nitrogen (N₂) adsorption test. N₂ adsorption measures the surface area, pore size and total pore volume of the material (Rouquerol et al. 2013; Thommes et al. 2015). The application of N₂ adsorption analysis and the mentioned

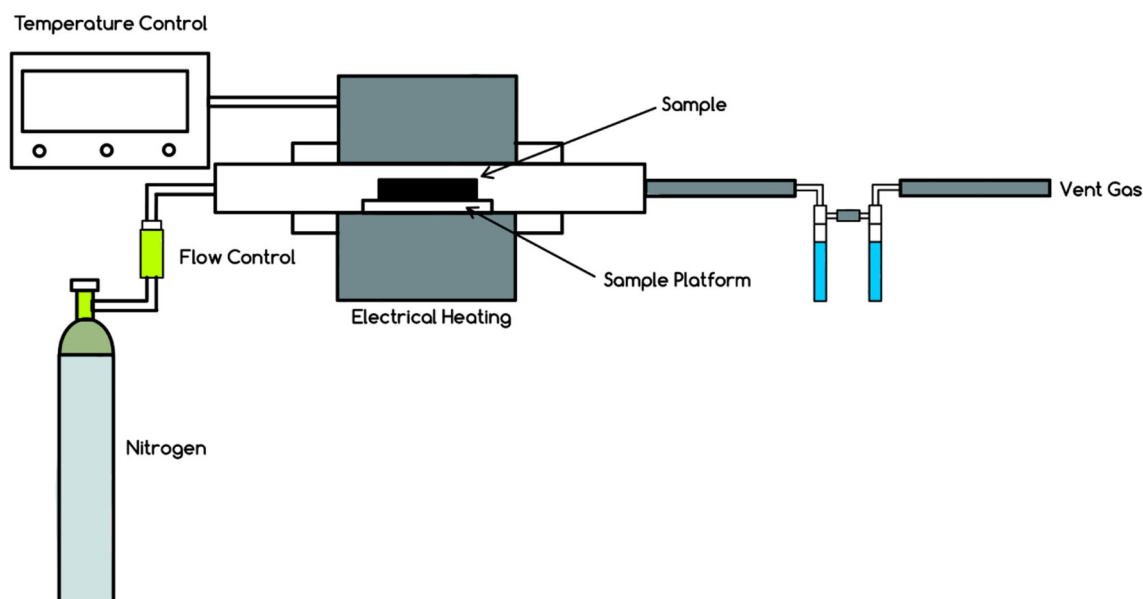


Fig. 2 Activated carbon preparation setup

Table 1 Structure and CCD design matrix of synthesis experiment

# Run	Coded factors		Actual factors	
	<i>T</i>	<i>W</i>	<i>T</i> (°C)	<i>W</i>
1	− 1	− 1	400	1
2	0	− 1	600	1
3	0	0	600	2.5
4	1	0	800	2.5
5	0	0	600	2.5
6	0	1	600	4
7	− 1	0	400	2.5
8	1	1	800	4
9	1	− 1	800	1
10	0	0	600	2.5
11	− 1	1	400	4
12	0	0	600	2.5
13	0	0	600	2.5

models in this study provides information on the porous structure and adsorption parameters of the material.

2.4.1 Brunauer–Emmett–Teller (BET) model

BET method is widely used in measuring surface area, total pore volume and pore size of porous materials (Rouquerol et al. 2013; Cohen 2007; Lowell et al. 2012). Linearized BET equation is as expressed in Eq. (4) (Rouquerol et al. 2013)

$$\frac{\frac{P}{P_o}}{n\left(1 - \frac{P}{P_o}\right)} = \frac{1}{n_m C} + \frac{C - 1}{n_m C} \left(\frac{P}{P_o}\right) \quad (4)$$

where n represents the quantity adsorbed at a relative pressure (P/P_o); n_m is the specific monolayer capacity. Based on BET theory, C has an exponential relationship with the monolayer adsorption energy. The value of C provides an indication of the isotherm shape within the BET range. The estimated value of BET specific area depends on conditions such as temperature, the adsorptive and method used in finding the pressure range when using the BET equation (Thommes et al. 2015).

2.4.2 Dubinin–Radushkevich (D–R) model

The D–R model equation can be expressed as:

$$\ln V = \ln V_o \left(- \left(\frac{A}{E} \right)^2 \right) \quad (5)$$

where V is the adsorbed volume; V_o is the limiting volume of adsorption; E is the characteristic energy of adsorption. The adsorption potential A is defined as:

$$A = RT \ln \left(\frac{P_s}{P} \right) \quad (6)$$

where R is gas constant; T is equilibrium temperature; P is pressure. The saturation pressure (P_s) is given by:

$$P = \left(\left(\frac{T}{T_c} \right)^2 \right) P_c \quad (7)$$

where P_c and T_c are the critical pressure and temperature of the adsorbate. Substituting Eq. (6) into (5) will give the generalized and linear expression of the D–R equation:

$$\ln V = \ln V_o - (RT/E)^2 \left(\ln \left(\frac{P_s}{P} \right) \right)^2 \quad (8)$$

A plot of $\left(\ln \left(\frac{P_s}{P} \right) \right)^2$ versus $\ln V$ will produce a straight line graph with the intercept yielding limiting micropore uptake, V_o , which gives the micropore volume given the density of the adsorbed phase.

2.4.3 Toth model

The methane and nitrogen experimental isotherms were correlated with Toth model widely used for Type 1 isotherms of gas physisorption on activated carbons (Saha et al. 2007; Akkimaradi et al. 2009; Martin et al. 2011; Thommes et al. 2015). Toth isotherm model adequately describes adsorption at low and high pressure. The form of Toth isotherm model used is as expressed in Eq. (9):

$$C = C_0 \left(\frac{k_0 \exp \left(\frac{H_{ads}}{RT} \right) P}{\left[1 + \left(k_0 \exp \left(\frac{H_{ads}}{RT} \right) P \right)^t \right]^{\frac{1}{t}}} \right) \quad (9)$$

where C is the amount of adsorbate adsorbed; C_0 is the saturated amount of adsorbate adsorbed; P is equilibrium pressure; k_0 is equilibrium constant; H_{ads} is the isosteric heat of adsorption; R is the gas constant, T is equilibrium temperature and t is a dimensionless constant that describes the heterogeneous nature of the adsorbent.

2.5 Characterization of the synthesised activated carbons

2.5.1 Gas sorption measurement

Nitrogen adsorption test was carried out at 77 K. 0.2 g of the activated carbon sample was degassed at 150 °C for 6 h in a Nitrogen flow using a Micromeritics Flow Prep 060 unit. The sample was transferred to a Micromeritics TriSta 3000 instrument for analysis. The nitrogen adsorption data was used to calculate (1) Surface area, S_{BET} , using BET method (Brunauer et al. 1938); (2) micropore volume, V_{DR} , using the Dubinin–Radushkevich (DR) method (Vyas and Kumar 2004); (3) total pore volume, V_T , determined at a relative pressure of $P/P_o = 0.99$ (Gregg et al. 1967); (4) mesopore volume, V_{me} , calculated as the difference $V_T - V_{DR}$.

2.5.2 SEM/EDS analyses

The surface morphology and elemental analysis of the synthesized activated carbon and discard coal was analyzed by scanning electron microscopy (SEM) technique using Carl Zeiss Sigma Field Emission Scanning Electron Microscope equipped with Oxford X-act EDS detector.

2.5.3 XRD analysis

X-ray powder diffraction analysis of the activated carbon was conducted using D2 PHASER Bruker Meas Srv D2-208365 with SSD 160 (1-D mode) for the response patterns, purity, and crystallography of the powdered activated carbon sample.

2.5.4 High-pressure adsorption

Measurement of methane and nitrogen adsorption capacity of the synthesized activated carbon with the highest surface area was measured at room temperature (25 °C) and pressures up to 4 Megapascal (MPa) using Particulate Systems High-Pressure Volumetric Analyzer (HPVA II) (Fig. 3). The equipment (HPVA II) utilizes the volumetric method in its analysis to produce high-pressure adsorption and desorption isotherms using different gases such as CH_4 , CO_2 , and H_2 (Particulate Systems 2011). In the volumetric method, a known volume of gas is introduced into the sample chamber for analysis. On attaining equilibrium between the sample and the gas, the final equilibrium pressure is noted. Calculating the amount of gas adsorbed by the sample is done using the equilibrium pressure data. The adsorption analysis is carried out repeatedly at specified pressure intervals until it reaches the maximum set

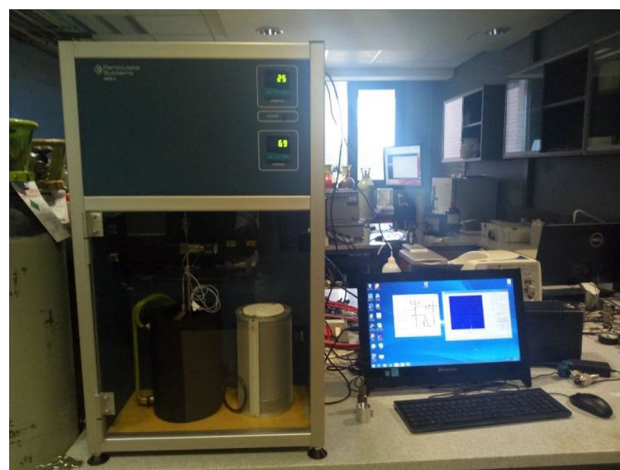


Fig. 3 Image of particulate systems high-pressure volumetric analyzer (HPVA II)

pressure. To obtain the adsorption isotherm, data of the quantity of gas adsorbed is plotted against the equilibrium pressure. In carrying the desorption analysis, the pressure is reduced steadily to obtain the desorption isotherms.

3 Results and discussion

3.1 Preliminary analysis of discard coal

The results of the proximate, ultimate, total sulfur content and BET surface area and porosity of the discard coal are presented in Table 2.

The result from the proximate analysis (adb) revealed that discard coal has a high ash content of 35.4% and fixed carbon accounting for less than 50%. The measured moisture content depicts the water present in coal. The percentage of moisture varies according to the rank of the coal, with highly ranked coals most often containing a higher percentage of moisture (Donahue and Rais 2009). The moisture content of the discard coal in this study is 2.1%. The ultimate analysis showed that the discard coal contains carbon content of 48.907%, total sulfur content of 1.34%, nitrogen content of 1.15% and hydrogen content of 2.67%. The oxygen content of the discard coal was found to be 8.44% using difference calculation. The surface area of discard coal was found to be 3.848 m²/g, pore volume of 0.014 cm³/g and pore size of 15 nm respectively.

Table 2 Properties of discard coal

Analysis	Discard coal
<i>Proximate analysis (wt%, adb)</i>	
Moisture content	2.1
Volatile matter	20
Fixed carbon	42.5
Ash	35.4
<i>Ultimate analysis (wt%, adb)</i>	
Carbon	48.90
Hydrogen	2.67
Nitrogen	1.15
Oxygen	8.44
Total sulfur (wt%, adb)	1.34
<i>Surface properties</i>	
BET surface area (m ² /g)	3.848
Pore volume (cm ³ /g)	0.014
Pore size (nm)	15.111

wt% weight percent, adb air-dried basis

3.2 Chemical and physical properties of the synthesized activated carbon

Chemical activation has been adjudged as the best method in producing activated carbon with well-developed porosity and large surface area when compared to physical activation method (Dai et al. 2006). In this section, the influence of factors such as temperature, type of chemical reagent, chemical reagent weight ratio and particle size on the surface area and porosity of the activated carbon are discussed.

3.2.1 Effect of activation temperature on the surface area and pore volume of the synthesized activated carbon

The textural properties of the synthesized activated carbon samples as obtained from nitrogen adsorption at 77 K is presented in Table 3. The influence of temperature on the properties of the activated carbon samples can be observed from the results shown in Table 3. It is evident from the results that, surface area and pore volume progressively increase with temperature, obtaining the highest surface area of 1826.41 m²/g at 800 °C. The surface area obtained is higher than some activated carbon produced from coal-based materials: Indonesian low grade coal—668 m²/g (Martin et al. 2011), commercial activated carbon—900 m²/g (CarboTech 2016), Illinois basin coal—1560 m²/g (Sun et al. 1997) and bituminous coal—1150 m²/g (Himeno et al. 2005). It has been reported that the temperature above 800 °C leads to poor reaction yield and poor narrow pore size distribution (Linares-Solano et al. 2012). To further buttress this point, from Eq. (3), alkaline carbonate is a product of the chemical activation reaction. At temperatures above 800 °C, decomposition of the alkaline carbonate takes place with CO₂ evolving as one of the products of decomposition as shown in Eq. (10):



The CO₂ from Eq. (10) will react with the remaining carbon leading to another activation reaction as a result of the reaction as shown in Eq. (2). This will cause further widening of the pores and reduction in reaction yield, thereby defeating the key advantages of hydroxide activation which includes high yield and narrow pore size distribution.

3.2.2 Effect of chemical reagent/weight ratio on the surface area and pore volume of the synthesized activated carbon

Preparation of activated carbon samples using alkaline hydroxides has been subject of various studies (Lozano-Castello et al. 2001; Lillo-Ródenas et al. 2001; Hu and

Table 3 Textural properties of activated carbons

Sample	Chemical weight ratio	Temperature (°C)	Surface area (m ² /g)	Total pore volume, V _T (cm ³ /g)	Micropore volume, V _{DR} (cm ³ /g)	Ratio, V _{DR} /V _T	Mesopore volume, V _{me} (V _T - V _{DR})
AC-1	1	400	143.84	0.220	0.063	0.29	0.157
AC-2	2.5	400	161.54	0.280	0.075	0.27	0.205
AC-3	4	400	258.00	0.440	0.079	0.18	0.361
AC-4	1	600	275.15	0.360	0.236	0.66	0.124
AC-5	2.5	600	463.67	0.612	0.181	0.30	0.431
AC-6	4	600	671.68	0.698	0.583	0.84	0.115
AC-7	1	800	1216.36	0.765	0.664	0.87	0.101
AC-8	2.5	800	1374.20	1.037	0.885	0.85	0.152
AC-9	4	800	1826.41	1.252	0.887	0.71	0.365

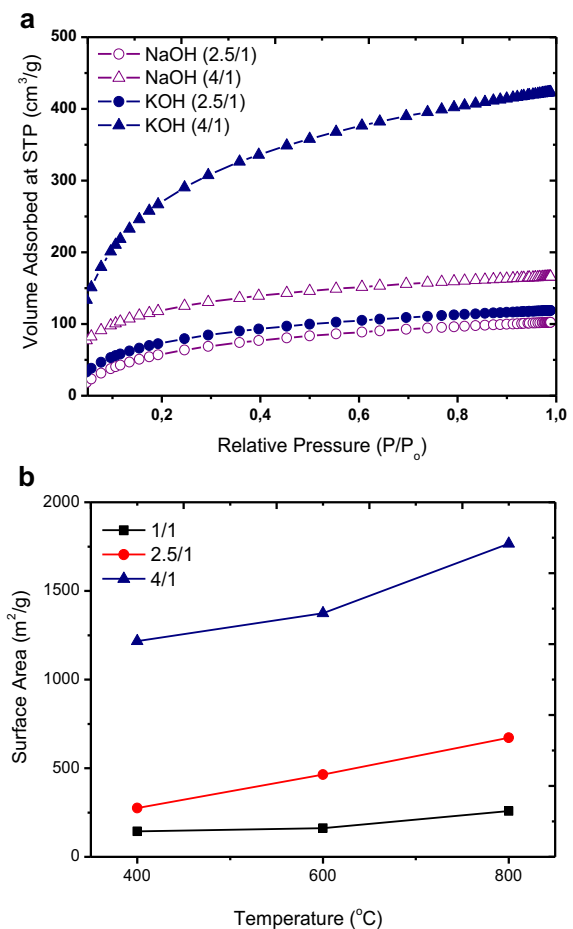
AC activated carbon

Table 4 Effect of choice of chemical reagent (NaOH and KOH) on the surface area and pore volume of activated carbons prepared from discard coal

Surface characteristic	Discard coal/chemical weight ratio			
	1:2.5		1:4	
	NaOH	KOH	NaOH	KOH
Surface area (m ² /g)	143.84	463.67	251.57	671.68
Pore volume (cm ³ /g)	0.159	0.612	0.257	0.698

Srinivasan 1999; Ahmadpour and Do 1996). Activated carbon prepared from NaOH or KOH has peculiar properties such as low ash content, high adsorption capacity and narrow pore distribution (Linares-Solano et al. 2012). Table 4 present the surface area and pore volume of activated carbons prepared using KOH and NaOH at different weight ratio at activation temperature of 600 °C. The significance of the nature of chemical agent used in activation can be observed; their response to activation consequently the adsorption capacity of the resulting activated carbon samples are different, on account of their distinct reactivity and structure (Linares-Solano et al. 2012).

As can be observed from Table 4, increasing the chemical weight ratio of KOH and NaOH OH increases the surface area and pore volume of the activated carbon samples. Increase in the chemical weight ratio increases the extent of reaction resulting in an increase in surface area and porosity. An increase in a weight ratio from 2.5 to 4 shows a 45% increase in surface area and a 15% increase in pore volume for KOH activated carbon. For the NaOH activated carbon, an increase in weight ratio resulted in a 75% increase in surface area and a 62% increase in pore volume. From the percent increment in the surface properties, an increase in chemical reagent weight ratio shows

**Fig. 4** Effect of the chemical reagent/weight ratio on **a** nitrogen adsorption isotherms **b** surface area of KOH activated carbons

an increase in the surface properties of KOH activated carbon and NaOH activated carbon with NaOH activated carbon having a higher percentage increase for both surface area and pore volume. KOH activated carbon showed

improved surface characteristics compared to NaOH activated carbon at the different chemical weight ratios used.

Figure 4 shows the effect of chemical reagent and weight ratio on nitrogen adsorption isotherms and the effect of weight ratio on the surface area of KOH activated carbon. As can be observed, an increase in the weight ratio of the chemical reagent results in an increase in surface area and an increase in the volume of gas adsorbed onto the activated carbon.

As can be seen from Table 4, KOH is noticeably more effective than NaOH in producing activated carbon in terms of surface area, pore volume and adsorption capacity. Activated carbon prepared with a weight ratio of 4 was observed to have the highest surface area and pore volume for both NaOH and KOH. This is in agreement with previous studies on activated carbon prepared from coal-based materials (Lozano-Castello et al. 2001; Jibril et al. 2007; Lillo-Ródenas et al. 2003; Linares-Solano et al. 2012; Sreńscek-Nazzal et al. 2013; Wu et al. 2005; Ahmadpour and Do 1996).

3.2.3 Effect of discard coal particle size on the surface area and pore volume of the synthesized activated carbon

The results of the surface area and pore volume of activated carbons produced from different particle sizes of discard coal using KOH activation is presented in Table 5. The activation experiment was conducted for particle sizes 0.15–0.25 mm, 0.25–0.5 mm and 0.5–1 mm at activation temperature of 800 °C and discard coal/KOH weight ratio of 1:4. As can be seen from Table 5, activated carbon from discard coal with larger particle size shows a decrease in surface area and pore volume. About 35% decrease in surface area was observed as the particle size increases from 0.15–0.25 mm to 0.25–0.5 mm and 51% further decrease was observed as the size is increased to 0.5–1 mm. The same observation hold for the pore volume as 37% and 46% decrease respectively was observed.

Figure 5 shows the nitrogen adsorption isotherms of the activated carbons from different particle sizes of discard coal. Discard coal of smaller particle sizes produces activated carbon with more N₂ adsorption capacity which is as a result of more developed porosity. This is because, in

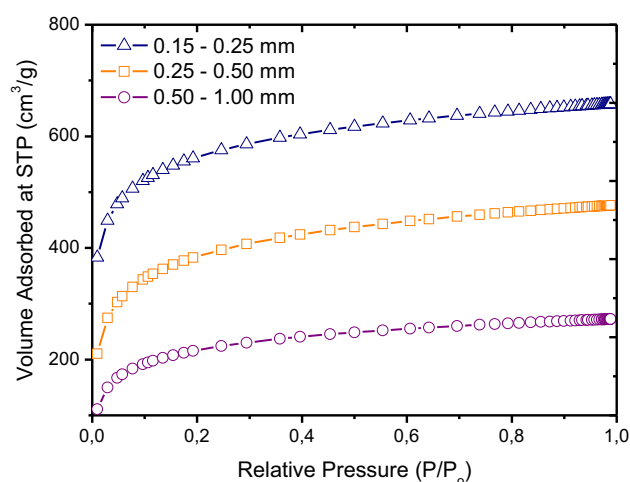


Fig. 5 Effect of discard coal particle size on nitrogen adsorption isotherm

larger particles, there is less exposure to the chemical reagent at the wall surfaces; therefore, smaller particle sizes with better exposure to the chemical reagent will have a better surface area and pore volume (Ahmadpour and Do 1996). Similarly, the smaller the particle sizes, the higher the diffusion rate of adsorbates into the pores, thereby improving kinetics and pore development.

3.3 Statistical analysis

The influence of the independent variables, activation temperature (T) and KOH weight ratio (W) on the surface area and pore volume of the synthesized activated carbons were analyzed in this section. Table 6 shows the results of the RSM fitting of the experimental data using ANOVA. The F-value and Prob. > F value are key pointers to the significance and the suitability of the model (Hou et al. 2013). F-value of 266 and 147 for surface area and pore volume respectively and prob. > F value less than 0.05 shows that the model is suitable and provides a good fit for the experimental data. High R^2 value close to 1 is required and indicates a good correlation between the experimental and observed data. The Pred. R^2 of 0.9792 and 0.9417 is in reasonable agreement with the Adj. R^2 of 0.9910 and 0.9839 for surface area and pore volume respectively. The

Table 5 Effect of discard coal particle sizes on the surface properties of the activated carbons

Particle size (mm)	Surface area (m ² /g)	Pore volume (cm ³ /g)	Pore size (nm)
0.15–0.25	1826.41	1.25	2.77
0.25–0.5	1179.9	0.79	3.13
0.5–1	582.4	0.42	3.26

Table 6 ANOVA results for surface area and pore volume of the synthesized activated carbons

Source	Sum of squares		DOF		Mean square		F-value		Prob. > F		Remark
	SA	PV	SA	PV	SA	PV	SA	PV	SA	PV	
Model	3.26E+06	0.97	5	5	6.53E+05	0.19	266	147	< 0.0001	< 0.0001	Sig.
T	2.48E+06	0.74	1	1	2.48E+06	0.74	1009	565.4	< 0.0001	< 0.0001	
W	2.09E+05	0.18	1	1	2.09E+05	0.18	85.3	138.2	< 0.0001	< 0.0001	
T × W	61476.72	0.018	1	1	61476.72	0.018	25.1	13.5	0.0016	0.0079	
T ²	3.72E+05	0.026	1	1	3.72E+05	0.026	151.5	20	< 0.0001	0.0029	
W ²	14465.52	2.80E−03	1	1	14465.52	2.80E−03	5.9	2.13	0.0456	0.1882	
Residual	17176.33	9.22E−03	7	7	2453.76	1.32E−03					Not Sig.
Lack of fit	5396.27	6.81E−03	3	3	1798.76	2.27E−03	0.61	3.77	0.6427	0.1164	
Pure error	11780.06	2.41E−03	4	4	2945.01	6.03E−04					
Cor Total	3.28E+06	0.98	12	12							
R ²	0.9948	0.9906									
Adj. R ²	0.9910	0.9839									
Pred. R ²	0.9792	0.9417									

SA, surface area; PV, pore volume; DOF, degree of freedom; T, temperature; W, KOH/discard coal weight ratio; R², correlation coefficient; Adj., adjusted; pred., predicted; sig., significant

p value as shown in Table 3 shows that the parameters, *T* and *W* are significant factors that influence the surface area and pore volume of the activated carbon samples.

A quadratic model was applied to evaluate the effect of the independent variables on the response parameters (surface area and pore volume). The model equation is expressed in terms of coded factors and actual factors as given in Eqs. (11)–(14).

Coded factor:

$$\begin{aligned} \text{Surface area} = & 414.99 + 642.27T + 186.79W \\ & + 123.97TW + 366.83T^2 + 72.37W^2 \end{aligned} \quad (11)$$

$$\begin{aligned} \text{Pore volume} = & 0.59 + 0.35T + 0.17W + 0.067TW \\ & + 0.098T^2 - 0.032W^2 \end{aligned} \quad (12)$$

Actual factor:

$$\begin{aligned} \text{Surface area} = & 2299.2 - 8.83T - 284.24W + 0.41TW \\ & + (9.17 \times 10^{-3} \times T^2) + 32.17W^2 \end{aligned} \quad (13)$$

$$\begin{aligned} \text{Pore volume} = & 0.37 - (1.72 \times 10^{-3} \times T) + 0.05W \\ & + (2.23 \times 10^{-4} \times T \times W) \\ & + (2.44 \times 10^{-6} \times T^2) - 0.01W^2 \end{aligned} \quad (14)$$

The 3D surface plots were analyzed to observe the influence of changing levels of the two process variables on the surface area and pore volume of the activated carbons. Figure 6a, b shows a similar effect of temperature and weight ratio on the surface area and pore volume of the activated carbons. An increase in temperature and weight

ratio showed a corresponding increase in surface area and pore volume.

Figure 7a, b shows the normal probability plot of residuals and plot of the predicted versus actual values of the two responses. The normal probability plot establishes if the residuals follow a normal distribution. The residuals measure the deviations between the predictions of the responses using the independent variables. From Fig. 7a, b, it is observed that the model gave a good approximation of the actual values of the responses. The normal probability plot of the residuals is approximately linear, an indication that the error terms are normally distributed. The predicted value versus actual value plot shows the actual measured response against the values predicted by the model. As observed, there is a robust correlation between the model's predictions and the actual values. The errors observed between the predicted and actual values are within the acceptable limit which confirms that the regression model for the two responses, surface area, and pore volume provides a good fit.

To obtain the optimal independent variables (*T* and *W*), a desirability function was employed with the goal of maximizing the surface area and pore volume. Table 7 lists the parameter setting for the desired target response.

The output objective criteria is a maximized surface area and pore volume. In applying the desirability function, the condition that gave the maximum desirability factor was taken as the optimum condition (Gopalakannan and Senthilvelan 2013).

Table 8 present optimum solutions. Solution 1 was selected for the independent variables, having the highest

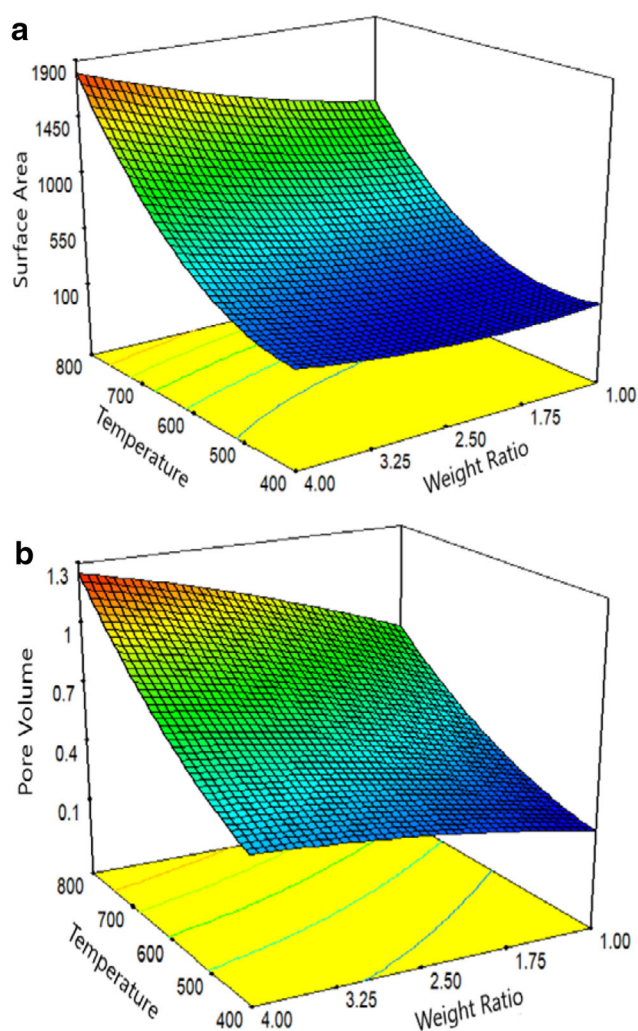


Fig. 6 3D surface plots showing the influence of temperature and weight ratio on **a** surface area and **b** pore volume

desirability value of 0.992. The highest possible surface area and pore volume were predicted in this region. The optimal independent variables or process conditions corresponds to a temperature of 800 °C and a weight ratio of 4.

Figure 8 shows the desirability plot and that of the responses. The plot shows the predicted values after optimization of 1807.21 m²/g and 1.2483 cm³/g for surface area and pore volume respectively. Generally, the result and analysis indicate the contribution of temperature and KOH weight ratio to the surface area and pore volume of the synthesized activated carbons. The optimized results are in good agreement with the experimental measurement, with an error percentage of 1% as calculated using Eq. 15:

Percentage of absolute error (POAE)

$$= \frac{\text{Experimental} - \text{Predicted}}{\text{Experimental}} \times 100 \quad (15)$$

3.4 Nitrogen adsorption analysis

Figure 9 shows the nitrogen adsorption isotherms of activated carbon samples synthesized from discard coal as obtained from the design of the experiment. The isotherms were observed to be of type I isotherm as classified by IUPAC classification (Thommes et al. 2015). The isotherms are characterized by volumes adsorbed at lower P/P_0 , followed by a knee showing characteristic of micropore development of wide pore diameter, and a horizontal plateau. It is observed from Fig. 9 that, the nitrogen adsorption capacity of the synthesized activated carbons differs greatly and it corresponds with the surface area which seems to govern its adsorption capacity. The higher the surface area, the higher the adsorption capacity of the activated carbon samples. This is in agreement with the results reported by Panella et al. (2005) and Bénard and Chahine (2007). The studies revealed that, for several carbon materials, adsorption capacity at 77 K corresponds with the surface area. Furthermore, Düren et al. (2004) applied computational methods to estimate adsorption capacity and surface areas of various carbon materials and found that the surface area is an important property of carbon materials that influences gas adsorption. The results from this study shows similar observations as shown in Fig. 9.

Table 9 shows the micropore volume of the activated carbon samples as obtained from fitting the nitrogen adsorption isotherms to the D–R model. The information obtained provides insight into the micropore structure of porous materials. The average correlation coefficient and standard error of estimate of 99.5% and 0.04% is an indication that the micropore volume obtained using D–R equation satisfactorily describes the micropore structure of the synthesized activated carbon samples.

3.4.1 Comparison of surface area result with previous studies

Table 10 shows the comparison of the highest surface area obtained from this study with surface area data of activated carbons prepared from coal materials as reported in the literature. As can be seen from Table 10, two activated carbons with higher surface area were obtained from anthracite coal. The surface areas are 31% and 14% higher than the highest surface area obtained from this study. This can be attributed to the high grade of anthracite coal when compared to the discard used in this study.

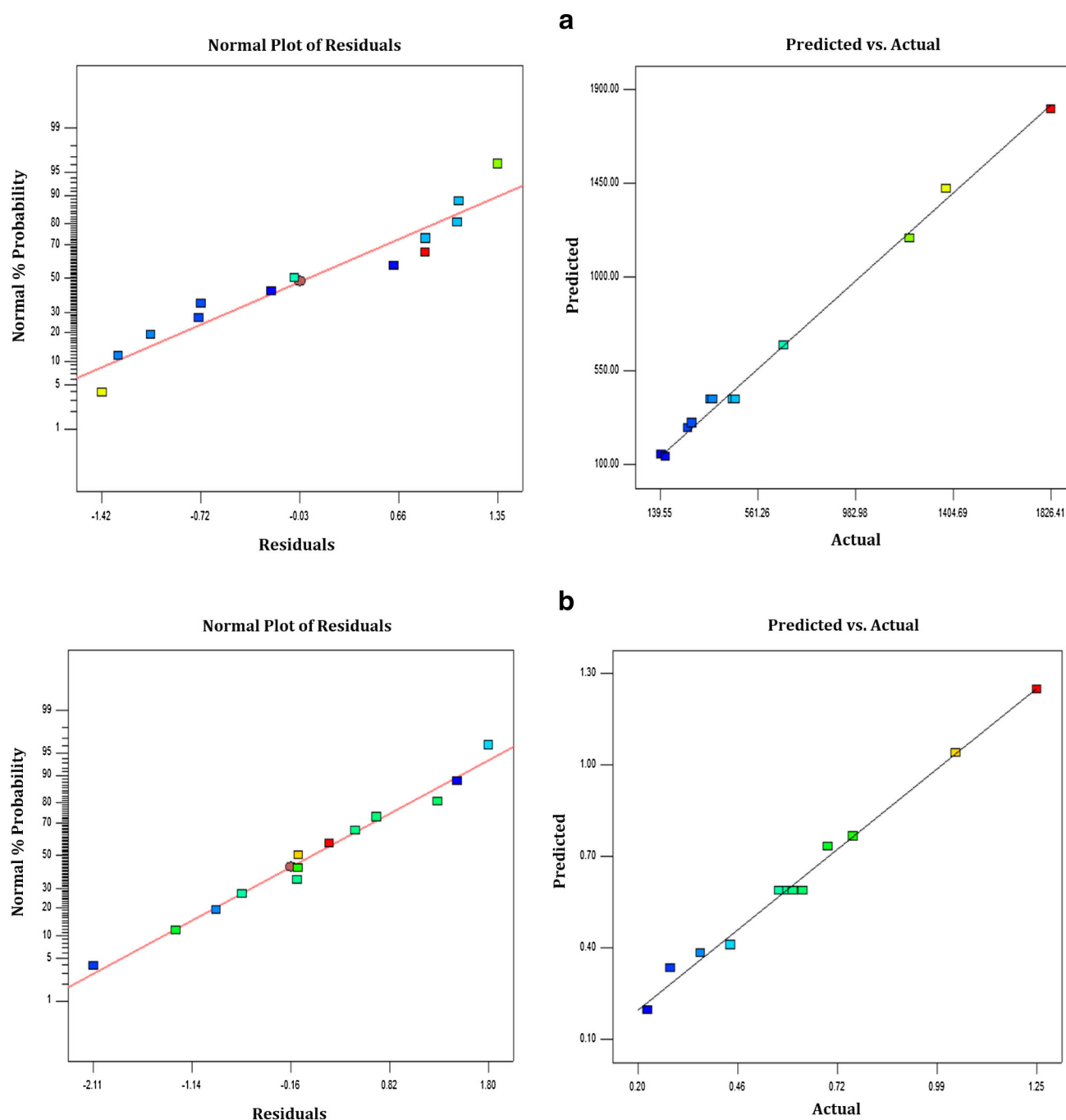


Fig. 7 Normal probability plot of residuals and plot of the predicted versus actual values of **a** surface area and **b** pore volume

Table 7 Optimum conditions setting for optimized response

Constraints	Goal	Lower limit	Upper limit
Temperature (<i>T</i>)	Is in range	400	800
Weight ratio (<i>W</i>)	Is in range	1	4
Surface area	Maximize	143.84	1826.41
Pore volume	Maximise	0.22	1.252

3.5 SEM/EDS analysis

SEM images of discard coal and its activated carbon are shown in Fig. 10. A thick wall structure with no visible cavities or pores can be observed from Fig. 10a. After activation of the discard coal with KOH, well-developed pores are seen clearly on the surface of the prepared activated carbon as shown in Fig. 10b. Pore development is a result of the reaction of KOH with discard coal during the

Table 8 Optimised solutions

Solution	Temperature (°C)	Weight ratio	Surface area (m ² /g)	Pore volume (cm ³ /g)	Desirability	Remark
1	800	4	1807.21	1.2483	0.992	Selected
2	789.98	4	1732.98	1.2178	0.956	
3	800	3.52	1670.22	1.1890	0.923	
4	800	3.5	1662.16	1.1851	0.919	

activation process. This is in line with the results reported by Lua and Yang (2004), Omri and Benzina (2012). The studies revealed that activation at 800 °C with KOH leads to significant pore development and volatiles removal. Furthermore, Lillo-Ródenas et al. (2003) and Linares-Solano et al. (2012) reported that, during the activation process, the diffusion of KOH molecules into the pores of the precursor material improves the KOH-carbon interaction, thereby leading to the creation of more pores. The pore development is very important as it increases the surface area and pore volume of the activated carbon. The SEM analysis confirms the development of a porous material in comparison to the discard coal.

The result of the energy-dispersive X-ray spectroscopy (EDS) analysis is shown in Fig. 11, revealing the composition of the elements present in the activated carbon. The result of the spectrum showed the presence of carbon and oxygen element on energy band of < 0.5 keV, while silicon is found on the energy band of < 2 keV. The EDS analysis reveals the presence of three elements (C, O, and Si) in the activated carbon with 77.62% of carbon, 15.52% of oxygen and 6.80% of silicon. The presence of Si in the activated carbon can be attributed to its corresponding presence in the ash content of the discard coal. The EDS analysis also shows no presence of potassium (K) in the activated carbon, this is an indication of the efficient washing of the activated carbon with hydrochloric acid (HCl) which totally remove all traces of potassium.

3.6 XRD analysis

Figure 12 reveals the XRD profile of discard coal and activated carbon derived from it. The profile reveals that discard coal contains inorganic compounds, hence the high crystallinity before activation with KOH. The XRD profile for discard coal (Fig. 12a) reveals the presence of inorganic contents with well-defined peaks observed at $2\theta = 13^\circ$, 21° , 27.6° , 39.3° and 60.8° . When compared to the profile for the activated carbon (Fig. 12b), it showed a broad diffraction background (broad peak observed at $2\theta = 43.2^\circ$) and the lack of well-defined peak is an indication of a predominantly amorphous structure as expected for organic materials (Wang and Lu 1997; Köseoğlu and

Akmil-Başar 2015). The pattern of the activated carbon sample displayed no distinct peaks associated with any crystalline phase. The XRD analysis shows us that the prepared activated carbon has lower inorganic constituents in comparison with the discard coal.

3.7 High-pressure adsorption analysis

3.7.1 Experimental results

The amount of methane and nitrogen adsorbed on the activated carbon with the highest surface area are presented in Table 11. The experimental data were obtained at pressures up to 4 MPa and at ambient temperature of 25 °C.

Figure 13 shows the experimental isotherms of methane and nitrogen adsorbed on the activated carbon. It is observed that the isotherm for both methane and nitrogen adsorption exhibit Type I IUPAC isotherm classification (Thommes et al. 2015). A sharp increase in the amount of gas adsorbed at lower pressures and a gradual increase as the pressure increases were observed for both gases. Based on the volume of gas adsorbed on the activated carbon, methane provided a higher volume of uptake compared to nitrogen. At a pressure of 3.7 MPa, 157.58 cm³/g of methane is adsorbed by the activated carbon while 74.10 cm³/g of nitrogen is adsorbed. This is in agreement with the study reported by Blanco et al. (2010). The study revealed that, for an activated carbon derived from coconut shell, the amount of methane adsorbed is higher than that of nitrogen.

3.7.2 Experimental isotherms correlation

The methane and nitrogen experimental isotherms were correlated with Toth model and fitted using non-linear regression as shown in Fig. 13. The corresponding adsorption parameters and correlation coefficient (R^2) are as shown in Table 12.

The R^2 value of about 0.99 for methane and nitrogen adsorption is an indication that the Toth model provides an appropriate and suitable fit to the experimental adsorption isotherms for both methane and nitrogen. Therefore, Toth

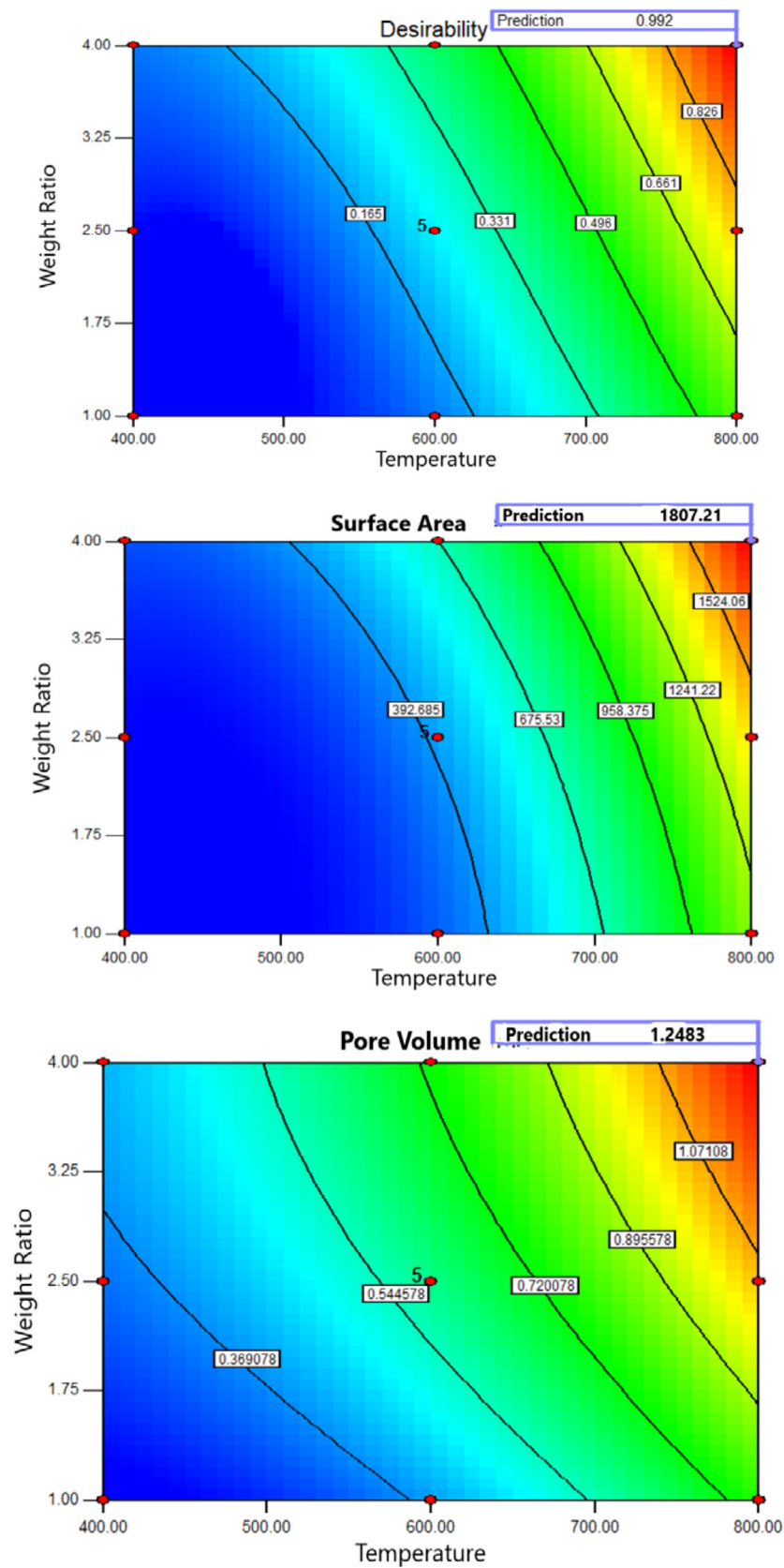


Fig. 8 Contour plot of desirability and responses

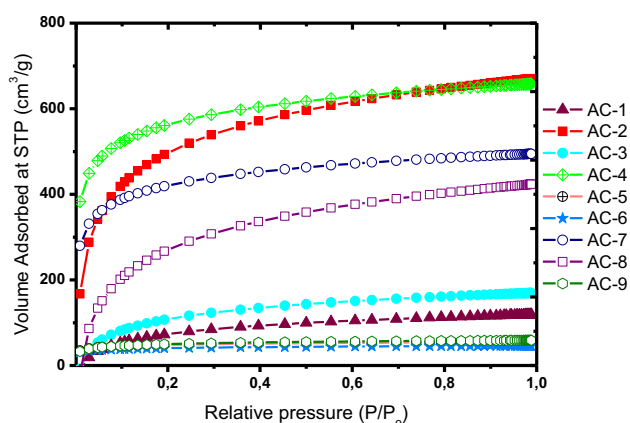


Fig. 9 Nitrogen adsorption isotherms of synthesized activated carbons

Table 9 Micropore volume calculated using the D-R equation

Activated carbons	V_{DR} (cm ³ /g)	R^2	SEE
AC-1	0.063	0.995	0.003
AC-2	0.075	0.995	0.003
AC-3	0.079	0.997	0.003
AC-4	0.236	0.995	0.042
AC-5	0.181	0.991	0.018
AC-6	0.583	0.996	0.010
AC-7	0.664	0.997	0.003
AC-8	0.885	0.999	0.005
AC-9	0.887	0.997	0.003

R^2 , coefficient of correlation; SEE, standard error of estimate

model can provide an accurate prediction of the uptake value of methane and nitrogen onto the synthesized activated carbon. The maximum methane and nitrogen adsorption capacity (C_0) as determined by the Toth model

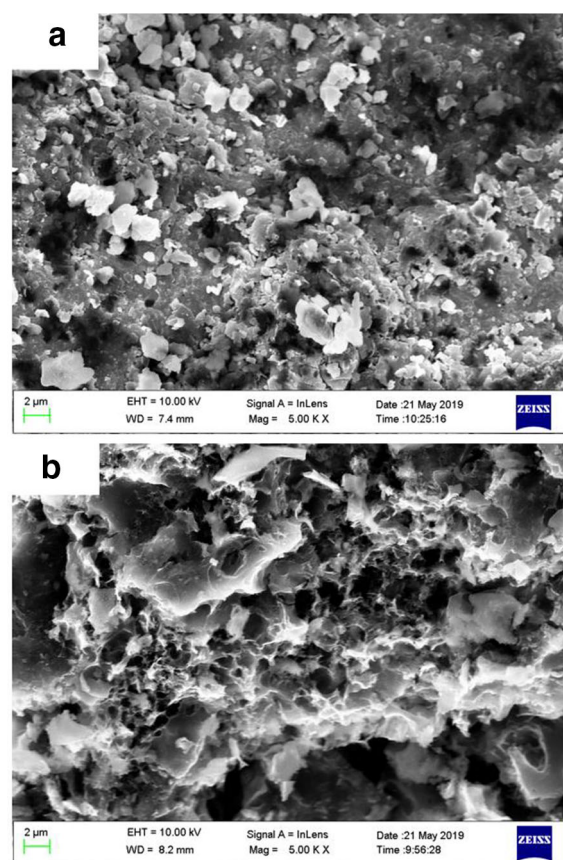


Fig. 10 SEM images of **a** discard coal and **b** activated carbon by KOH activation

were observed to be close to the maximum adsorbed experimental value. As can be seen from Table 12, methane adsorption has a higher isosteric heat of adsorption (H_{ads}) when compared to that of nitrogen adsorption. This suggests that more methane molecules penetrate into the pores of the activated carbon resulting in a stronger interaction between methane and the activated carbon

Table 10 Surface area of activated carbons produced from coal materials

S. no.	Activated carbon source	Surface area (m ² /g)	Reference
1	Blackwater coal from Queensland's Bowen Basin, Australia	1401	Gao et al. (2017)
2	Indonesian low-grade coal	668	Martin et al. (2017)
3	mineral coal (commercial activated carbon)	900	CarboTech (2016)
4	An Illinois Basin coal	1560	Sun et al. (1997)
5	Anthracite coal	2085	Lozano-Castello et al. (2002b)
6	Bituminous coal	1150	Himeno et al. (2005)
7	Ning Xia anthracite coal, China	2398.1	Zou and Han (2001)
8	South African bituminous coal	350	Campbell et al. (2012)
9	South Africa discard coal	1826.41	This study

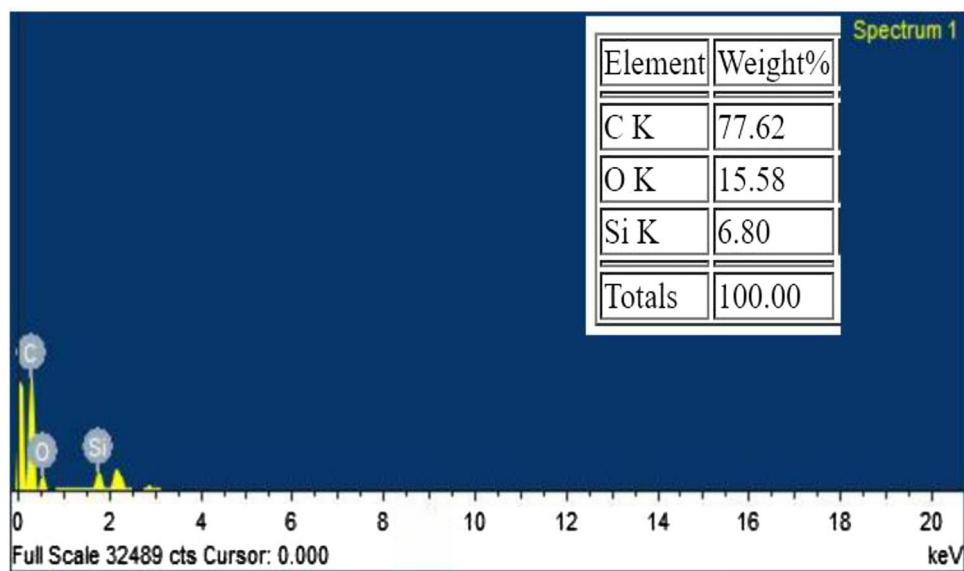


Fig. 11 EDS analysis spectrum of activated carbon from discard coal

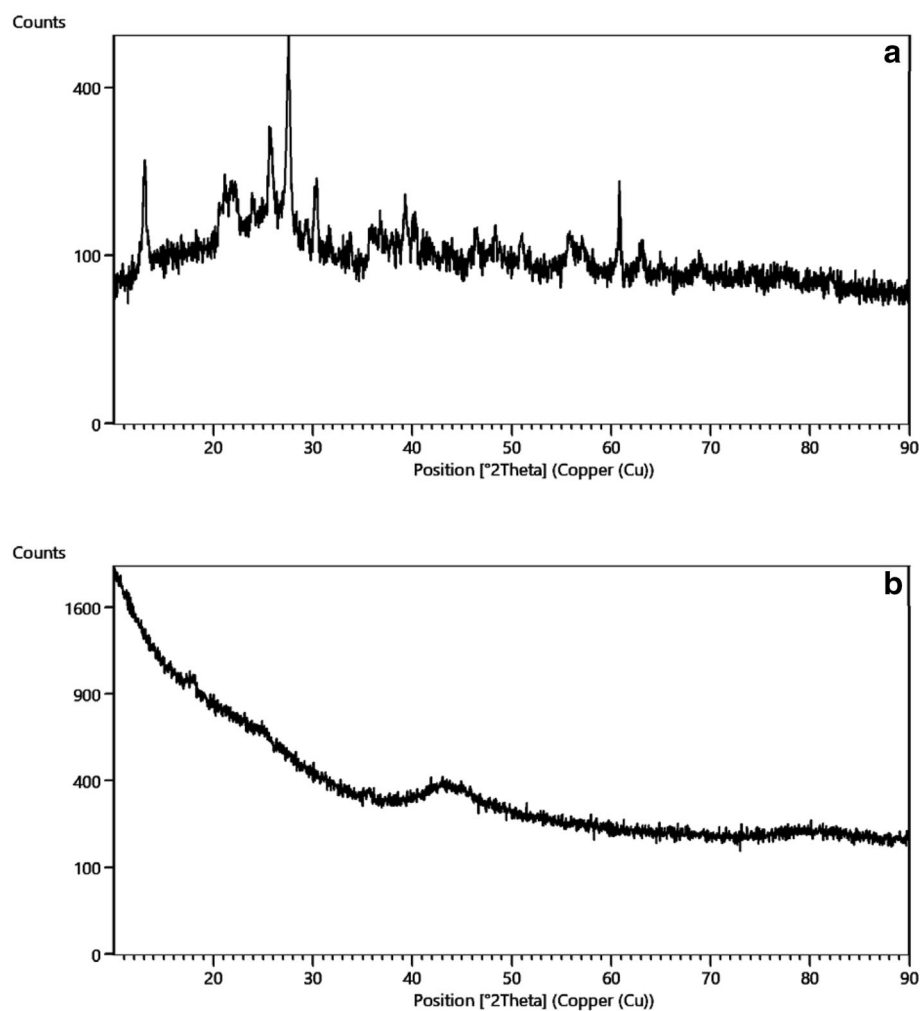
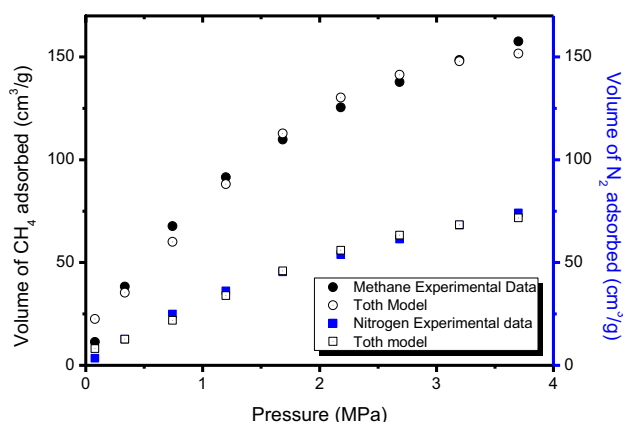


Fig. 12 XRD Profile of **a** discard coal sample and **b** activated carbon from discard coal

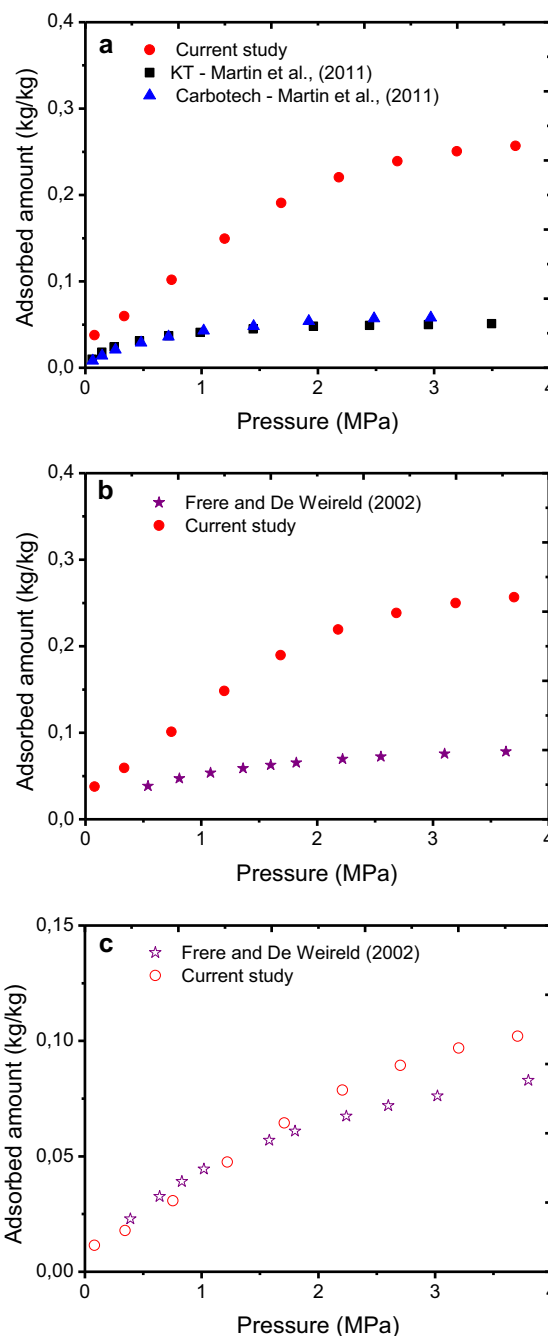
Table 11 Experimental data of nitrogen and methane adsorption

Methane		Nitrogen	
P (MPa)	Q (cm ³ /g)	P (MPa)	Q (cm ³ /g)
T = 25 °C			
0.1	11.41	0.1	3.41
0.3	38.34	0.3	12.72
0.7	67.71	0.8	24.92
1.2	91.46	1.2	36.17
1.7	109.82	1.7	45.45
2.2	125.46	2.2	53.87
2.7	137.85	2.7	61.39
3.2	148.55	3.2	68.15
3.7	157.58	3.7	74.10

**Fig. 13** Experimental and Toth model isotherms of methane and Nitrogen adsorption at high pressure**Table 12** Methane and nitrogen adsorption isotherm parameters for Toth equation

Toth parameters	Methane	Nitrogen
C_o (cm ³ /g)	156.15	77.25
k_o (MPa ⁻¹)	59.20	58.57
H_{ads} (kJ/mol)	16.22	14.47
t	0.184	0.169
R^2	0.9868	0.9900

hence a higher H_{ads} . The isosteric heat of adsorption (H_{ads}) obtained for methane adsorption is comparable to previous studies, 14.7–15.1 kJ/mol (Martin et al. 2011) and 11.97–13.39 kJ/mol (Loh et al. 2010). The Toth adsorption parameters provide useful information in the design of an appropriate gas storage system.

**Fig. 14** Comparison of the adsorbed amount with earlier studies: **a** methane adsorption at 27 °C, **b** methane adsorption at 30 °C and **c** nitrogen adsorption at 30 °C

3.7.3 Comparison of methane and nitrogen adsorption result with previous studies

The uptake amount of nitrogen and methane on activated carbon synthesized in this study is compared with methane and nitrogen adsorption data on activated carbon synthesized from low-grade coal and two commercial activated carbons (Martin et al. 2011; Frère and De Weireld 2002).

These are shown in Fig. 14a–c for methane at two different temperatures and nitrogen respectively. It is observed from Fig. 14a that methane adsorbed on activated carbon from low-grade coal and commercial activated carbon, carbotech (Martin et al. 2011) is about 80.5% and 70.6% lower than the current study for the same temperature respectively. In Fig. 14b, commercial activated carbon (chemviron carbon) adsorption data from Frère and De Weireld (2002) is compared with the present study. The adsorbed amount data plotted in Fig. 14b for the current study are predicted at the same temperature of 30 °C as the Frère and De Weireld (2002) using the Toth isotherm model for a realistic comparison. The methane adsorbed on chemviron carbon is about 76.2% lower than the current study for the same temperature. Similarly, as shown in Fig. 14c, nitrogen adsorbed on chemviron carbon is about 19% lower than nitrogen adsorbed on the activated carbon under study at same temperature and pressure. The likely reason for the difference in adsorbed amount is the textural properties of the mentioned activated carbons which are significantly lower than the textural properties of the activated carbon under study. Activated carbon from low grade coal and carbotech have surface area of 885 m²/g, 668 m²/g and pore volume of 0.47 cm³/g and 0.514 cm³/g respectively (Martin et al. 2011) while chemviron carbon has surface area of 993.5 m²/g and pore volume of 0.497 cm³/g (Frère and De Weireld 2002).

4 Conclusion

The results from this study establish that discard coal from coal beneficiation process is a good raw material to produce highly porous activated carbon. This study also established a positive correlation between surface area and adsorption capacity of activated carbon. The textural properties obtained from characterization gave an insight into the potential of activated carbon from discard coal in gas storage application. Methane adsorption on the activated carbon derived from discard coal was measured at conditions expected for ANG storage system, which is pressure up to 3.5 MPa and temperature of 25 °C. Methane and nitrogen adsorption data and similar data from literature showed that the activated carbon from discard coal provides higher adsorption in comparison with comparable adsorbents. Toth model was used to validate methane and nitrogen adsorption isotherms with an average of 0.99 coefficient of correlation. The parameters obtained from the Toth model are useful in the design of an efficient ANG storage system.

Acknowledgements This study was financially supported by Sustainable Energy and Environment Research Unit (SEERU),

University of the Witwatersrand and National Research Foundation (NRF) of South Africa, SARCHI Clean Coal Technology Grant (Grant Number: 86421). Opinions, findings, and conclusions stated are those of the authors and are not necessarily to be attributed to the NRF. This work is part of a PhD study in the School of Chemical and Metallurgical Engineering at the University of the Witwatersrand.

Open Access This article is distributed under the terms of the Creative Commons Attribution 4.0 International License (<http://creativecommons.org/licenses/by/4.0/>), which permits unrestricted use, distribution, and reproduction in any medium, provided you give appropriate credit to the original author(s) and the source, provide a link to the Creative Commons license, and indicate if changes were made.

References

- Ahmadpour A, Do D (1996) The preparation of active carbons from coal by chemical and physical activation. *Carbon* 34:471–479
- Akkimaradi BS, Prasad M, Dutta P, Saha BB, Srinivasan K (2009) Adsorption of nitrogen on activated carbon-refit of experimental data and derivation of properties required for design of equipment. *J Chem Eng Data* 54:2291–2295
- Alcañiz-Monge J, Lozano-Castelló D, Cazorla-Amorós D, Linares-Solano A (2009) Fundamentals of methane adsorption in microporous carbons. *Microporous Mesoporous Mater* 124:110–116
- Bandosz TJ, Ania C (2006) Surface chemistry of activated carbons and its characterization. In: Bandosz TJ (ed) *Interface science and technology*. Elsevier, Amsterdam
- Belaid M, Falcon R, Vainikka P, Patsa K (2013) Potential and technical basis for utilising coal beneficiation discards in power generation by applying circulating fluidised bed boilers. In: 2nd international conference on chemical, ecology and environmental sciences, June, pp 17–18
- Bénard P, Chahine R (2007) Storage of hydrogen by physisorption on carbon and nanostructured materials. *Scr Mater* 56:803–808
- Blanco AG, De Oliveira JA, López R, Moreno-Piraján J, Giraldo L, Zgrablich G, Sapag K (2010) A study of the pore size distribution for activated carbon monoliths and their relationship with the storage of methane and hydrogen. *Colloids Surf A* 357:74–83
- Brunauer S, Emmett PH, Teller E (1938) Adsorption of gases in multimolecular layers. *J Am Chem Soc* 60:309–319
- Campbell Q, Bunt J, Kasaini H, Kruger D (2012) The preparation of activated carbon from South African coal. *J South Afr Inst Min Metall* 112:37–44
- Carbotech (2016) CarboTech DGF 4 technical information. CarboTech AC GmbH, Essen
- Celzard A, Fierro V (2005) Preparing a suitable material designed for methane storage: a comprehensive report. *Energy Fuels* 19:573–583
- Center for Environmental Rights (2015) In pictures: What coal is doing to the Mpumalanga Highveld. <https://cer.org.za/news/in-pictures-what-coal-is-doing-to-the-mpumalanga-highveld>. Accessed 25 Mar 2018
- Cohen ER (2007) Quantities, units and symbols in physical chemistry. Royal Society of Chemistry, Cambridge
- Dai X-D, Liu X-M, Qian L, Yan Z-F, Zhang J (2006) A novel method to synthesize super-activated carbon for natural gas adsorptive storage. *J Porous Mater* 13:399–405
- Donahue CJ, Rais EA (2009) Proximate analysis of coal. *J Chem Educ* 86:222

- Düren T, Sarkisov L, Yaghi OM, Snurr RQ (2004) Design of new materials for methane storage. *Langmuir* 20:2683–2689
- Frère MG, De Weireld GF (2002) High-pressure and high-temperature excess adsorption isotherms of N₂, CH₄, and C₃H₈ on activated carbon. *J Chem Eng Data* 47:823–829
- Gao S, Ge L, Rufford TE, Zhu Z (2017) The preparation of activated carbon discs from tar pitch and coal powder for adsorption of CO₂, CH₄ and N₂. *Microporous Mesoporous Mater* 238:19–26
- Gopalakannan S, Senthilvelan T (2013) Application of response surface method on machining of Al–SiC nano-composites. *Measurement* 46:2705–2715
- Gregg SJ, Sing KSW, Salzberg H (1967) Adsorption surface area and porosity. *J Electrochem Soc* 114:279C–279C
- Himeno S, Komatsu T, Fujita S (2005) High-pressure adsorption equilibria of methane and carbon dioxide on several activated carbons. *J Chem Eng Data* 50:369–376
- Hou P, Cannon FS, Nieto-Delgado C, Brown NR, Gu X (2013) Effect of preparation protocol on anchoring quaternary ammonium/epoxide-forming compound into granular activated carbon for perchlorate adsorption: enhancement by Response Surface Methodology. *Chem Eng J* 223:309–317
- Hsu L-Y, Teng H (2000) Influence of different chemical reagents on the preparation of activated carbons from bituminous coal. *Fuel Process Technol* 64:155–166
- Hu Z, Srinivasan M (1999) Preparation of high-surface-area activated carbons from coconut shell. *Microporous Mesoporous Mater* 27:11–18
- Jibril BY, Al-Maamari RS, Hegde G, Al-Mandhary N, Houache O (2007) Effects of feedstock pre-drying on carbonization of KOH-mixed bituminous coal in preparation of activated carbon. *J Anal Appl Pyrol* 80:277–282
- Judd R, Gladding D, Hodrien R, Bates D, Ingram J, Allen M (1998) The use of adsorbed natural gas technology for large scale storage. Preprint symposium American Chemical Society Division of Fuel Chemistry, ACS, pp 575–579
- Köseoğlu E, Akmil-Başar C (2015) Preparation, structural evaluation and adsorptive properties of activated carbon from agricultural waste biomass. *Adv Powder Technol* 26:811–818
- Lillo-Ródenas M, Lozano-Castelló D, Cazorla-Amorós D, Linares-Solano A (2001) Preparation of activated carbons from Spanish anthracite: II. Activation by NaOH. *Carbon* 39:751–759
- Lillo-Ródenas M, Cazorla-Amorós D, Linares-Solano A (2003) Understanding chemical reactions between carbons and NaOH and KOH: an insight into the chemical activation mechanism. *Carbon* 41:267–275
- Linares-Solano A, Lillo-Ródenas M, Marco-Lozar JP, Kunowsky M, Romero-Anaya AJ (2012) NaOH and KOH for preparing activated carbons used in energy and environmental applications. *Int J Energy Environ Econ* 20:355
- Loh WS, Rahman KA, Chakraborty A, Saha BB, Choo YS, Khoo BC, Ng KC (2010) Improved isotherm data for adsorption of methane on activated carbons. *J Chem Eng Data* 55:2840–2847
- Lowell S, Shields JE, Thomas MA, Thommes M (2012) Characterization of porous solids and powders: surface area, pore size and density. Springer, Berlin
- Lozano-Castello D, Lillo-Ródenas M, Cazorla-Amorós D, Linares-Solano A (2001) Preparation of activated carbons from Spanish anthracite: I. Activation by KOH. *Carbon* 39:741–749
- Lozano-Castello D, Alcaniz-Monge J, De La Casa-Lillo M, Cazorla-Amorós D, Linares-Solano A (2002a) Advances in the study of methane storage in porous carbonaceous materials. *Fuel* 81:1777–1803
- Lozano-Castello D, Cazorla-Amorós D, Linares-Solano A (2002b) Powdered activated carbons and activated carbon fibers for methane storage: a comparative study. *Energy Fuels* 16:1321–1328
- Lua AC, Yang T (2004) Effect of activation temperature on the textural and chemical properties of potassium hydroxide activated carbon prepared from pistachio-nut shell. *J Colloid Interface Sci* 274:594–601
- Makal TA, Li J-R, Lu W, Zhou H-C (2012) Methane storage in advanced porous materials. *Chem Soc Rev* 41:7761–7779
- Marsh H, Reinoso FR (2006) Activated carbon. Elsevier, Amsterdam
- Martin A, Loh WS, Rahman KA, Thu K, Surayawan B, Alhamid MI, Ng KC (2011) Adsorption isotherms of CH₄ on activated carbon from Indonesian low grade coal. *J Chem Eng Data* 56:361–367
- Martin A, Idrus Alhamid M, Nasruddin, Suryawan B, Soong Loh W, Bin Ismail A, Chun W, Choon Ng K (2017) High-pressure adsorption isotherms of carbon dioxide and methane on activated carbon from low-grade coal of Indonesia. *Heat Transf Eng* 38:396–402
- Matranga KR, Myers AL, Glandt ED (1992) Storage of natural gas by adsorption on activated carbon. *Chem Eng Sci* 47:1569–1579
- Mills S (2018) The use of coal-derived wastes as a source of energy. IEA Clean Coal Center, London
- Morris RE, Wheatley PS (2008) Gas storage in nanoporous materials. *Angew Chem Int Ed* 47:4966–4981
- North B, Engelbrecht A, Oboirien B (2015) Feasibility study of electricity generation from discard coal. *J South Afr Inst Min Metall* 115:573–580
- Omri A, Benzina M (2012) Characterization of activated carbon prepared from a new raw lignocellulosic material: Ziziphus spina-christi seeds. *Journal de la Société Chimique de Tunisie* 14:175–183
- Onifade M, Genc B (2018) Modelling spontaneous combustion liability of carbonaceous materials. *Int J Coal Sci Technol* 5:191–212
- Panella B, Hirscher M, Roth S (2005) Hydrogen adsorption in different carbon nanostructures. *Carbon* 43:2209–2214
- Particulate Systems (2011) High pressure volumetric analyzer. Operator's manual. In: Micromeritics (ed). HPVA Series, Georgia, U.S.A
- Piechura H (2014) Application of Doosan Lentjes' CFB technology to discard coals. *S Afr J Chem Eng* 19:99–111
- Rouquerol J, Rouquerol F, Llewellyn P, Maurin G, Sing KS (2013) Adsorption by powders and porous solids: principles, methodology and applications. Academic Press, New York
- Saha BB, Koyama S, El-Sharkawy II, Habib K, Srinivasan K, Dutta P (2007) Evaluation of adsorption parameters and heats of adsorption through desorption measurements. *J Chem Eng Data* 52:2419–2424
- Schroeder A (2015) 2015 natural gas vehicle research roadmap. California Energy Commission, Sacramento
- Sreńscek-Nazzal J, Kamińska W, Michalkiewicz B, Koren ZC (2013) Production, characterization and methane storage potential of KOH-activated carbon from sugarcane molasses. *Ind Crops Prod* 47:153–159
- Sun J, Hippo E, Marsh H, O'Brien W, Crelling J (1997) Activated carbon produced from an Illinois basin coal. *Carbon* 35:341–352
- Thommes M, Kaneko K, Neimark AV, Olivier JP, Rodriguez-Reinoso F, Rouquerol J, Sing KS (2015) Physisorption of gases, with special reference to the evaluation of surface area and pore size distribution (IUPAC Technical Report). *Pure Appl Chem* 87:1051–1069
- Torregrosa-Rodríguez P, Martínez-Escandell M, Rodríguez-Reinoso F, Marsh H, De Salazar CG, Palazón ER (2000) Pyrolysis of petroleum residues: II. Chemistry of pyrolysis. *Carbon* 38:535–546
- Vyas RK, Kumar S (2004) Determination of micropore volume and surface area of zeolite molecular sieves by DR and DA equations: a comparative study. *Indian J Chem Technol* 11:704–709

- Wang S, Lu G (1997) Effects of oxide promoters on metal dispersion and metal-support interactions in Ni catalysts supported on activated carbon. *Ind Eng Chem Res* 36:5103–5109
- Wu F-C, Tseng R-L, Juang R-S (2005) Preparation of highly microporous carbons from fir wood by KOH activation for adsorption of dyes and phenols from water. *Sep Purif Technol* 47:10–19
- Zhao W, Fierro V, Zlotea C, Aylon E, Izquierdo M, Latroche M, Celzard A (2011) Optimization of activated carbons for hydrogen storage. *Int J Hydrogen Energy* 36:11746–11751
- Zou Y, Han B-X (2001) High-surface-area activated carbon from Chinese coal. *Energy Fuels* 15:1383–1386